MEASUREMENT OF CTE CHANGE IN COMPOSITE LAMINATE UNDER SPACE ENVIRONMENT USING FIBER OPTIC SENSORS

Sang-Guk Kang, Dong-Hoon Kang, Chun-Gon Kim* and Chang-Sun Hong

Department of Aerospace Engineering
Korea Advanced Institute of Science and Technology
373-1 Kusong-dong, Yusong-gu, Taejon, 305-701, South Korea
e-mail: cgkim@kaist.ac.kr

SUMMARY : In this research, the change of coefficient of thermal expansion (CTE) of graphite/epoxy composite laminate under space environment was measured using fiber optic sensors. Two fiber Bragg grating (FBG) sensors have been adopted for the simultaneous measurement of thermal strain and temperature. Low earth orbit (LEO) conditions with high vacuum, ultraviolet and thermal cycling environments were simulated in a thermal vacuum chamber. As a pre-test, a FBG temperature sensor was calibrated and a FBG strain sensor was verified through the comparison with the electric strain gauge (ESG) attached on an aluminum specimen in the same temperature range with the thermal cycling. The change of the CTE in composite laminate exposed to space environment was measured for intervals of aging cycles in real time. As a whole, there was no abrupt change of the CTE after 1000 aging cycles. After aging, however, the CTE decreased a little all over the test temperature range. These changes are caused by outgassing, moisture desorption, matrix cracking etc.

KEYWORDS : Fiber Optic Sensor, Smart Composites, Space Environment, Thermal Cycling

INTRODUCTION

Structures for aerospace use require high specific stiffness, high specific strength and low coefficient of thermal expansion (CTE) due to unusual ‘space environment’ they encounter. They must also accomplish assigned missions for long term even if they undergo dynamic loads in the procedure of testing, launching and severe environments such as extreme temperature change and vacuum. The polymer matrix composite is a compromising candidate for these conditions. Above all, graphite/epoxy composites have been successfully adapted in the wide fields of aerospace and other industries since 1970’s.

One of the most important functional requirements in the design of space structures is that materials used must have the coefficients of thermal expansion near to ‘zero’, which is directly related to dimensional stability of structures. In the design process, therefore, it is necessary to study on the change of CTE of structures as the aging proceeds when they are exposed to space environment for long term. Also, when the vehicle is being operated in

space, it's an important factor to confirm its health status as checking temperature and strain in real-time to complete its mission. The fiber optic sensor, which is actively being studied nowadays, is a suitable one for real-time health monitoring. Besides, it has many advantages when compared to conventional sensors such as the strain gauge and the thermocouple: it is immune to electromagnetic interference (EMI) and it has very small size, so it's easy to be embedded into structures. However, the systematic study on reliability of fiber optic sensor under the environment condition must be preceded. In this paper, the verification just for temperature was performed, for the other space environmental factors were insignificant to CTE change and were excluded by embedding fiber optic sensor in composite material.

FIBER BRAGG GRATING SENSOR

In this research, fiber Bragg grating sensor was used for the measurement of thermal strain. The grating was formed at the core of GeO_2 doped optical fiber by exposing the fiber to UV laser in the vicinity of 248 *nm* to optical fiber and making repetitive layers whose refractive index of core changes continuously with distribution of interference pattern of the laser. When the light with broadband source passes through Bragg grating, the light whose wavelength satisfies Bragg condition as equation (1) is reflected at the grating part.

$$\lambda_B = 2n_e\Lambda \qquad (1)$$

where n_e is effective refractive index of the fiber optic core with gratings and Λ is the grating period carved in core of optical fiber. In equaion (1), Bragg wavelength (λ_B) reflected at the gratings is the function of refractive index and grating period. And refractive index and grating periods are the function of temperature and strain, respectively, so when temperature and strain in the Bragg grating are disturbed, the resultant wavelength shift occurs. By differentiating Bragg condition equation and inserting the equations about temperature, strain, grating period, effective refractive index into the results, equation (2) is attained. From detecting the shifted Bragg wavelength precisely, we can measure the temperature and strain. through equation (2), which is the basic principle of FBG used as sensor.

$$\Delta\lambda_B = \lambda_B[(\alpha_f + \xi_f)\Delta T + (1 - P_e)\varepsilon] \qquad (2)$$

where P_e is photoelastic constant and expressed as follows.

$$p_e = \left(\frac{n_e^{\,2}}{2}\right)[p_{12} - \nu(p_{11} + p_{12})] \qquad (3)$$

In equation (2), α_f is thermal expasion coefficient of fiber optic and ξ_f is thermo-optic coefficient that means the change of refractive index of optical fiber with temperature. And p_{11} and p_{12} are strain-optic constants and ν is Poisson's ratio of optical fiber. P_e is known to have the value about 0.22 in case of gemanosilicate galss, but the strain must be measured strictly for the exact value of P_e because it can vary as optical fiber. In equation (2) wavelength shift occurs by both temperature and strain.

If the grating part is strain free and just undergoes temperature change, that is $\varepsilon = 0$, equation (2) can be rerewritten as following.

$$\Delta T = \frac{1}{\alpha_f + \xi_f} \cdot \frac{\Delta \lambda_B}{\lambda_B} \qquad (4)$$

Also, in case that FBG undergoes thermal strain, the resultant wavelength shift can be expressed as the summation of wavelength shifts by two terms: one is caused by refractive index change of optical fiber and the other by thermal strain of the structure as temperature changes. And this can be expressed like equation (5).

$$\frac{\Delta \lambda_B}{\lambda_B} = \xi_f \Delta T + (1 - P_e)(\alpha_{str} \Delta T) \qquad (5)$$

In equation (5), $\alpha_{str}\Delta T$ is thermal strain of the structure and it can be rearranged as following equation.

$$\varepsilon_{str} = \frac{1}{1 - P_e}\left[\frac{\Delta \lambda_B}{\lambda_B} - \xi_f \Delta T\right] \qquad (6)$$

FBG SENSOR RELIABLITY TEST AT HIGH AND LOWTEMPERATURE

FBG SENSORS AND SENSOR SYSTEM

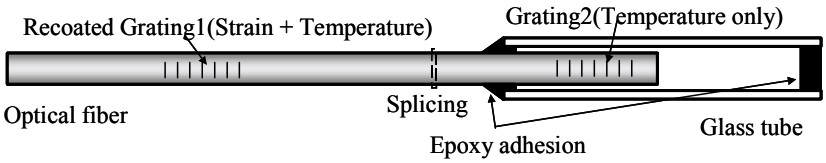

Fig. 1 FBG temperature and strain sensors.

Fig.1 shows the sensor used in this paper which is composed of two parts. One is for the measurement of thermal strain of the structure (grating 1) and the other is only for temperature (grating 2).

Grating 1 was recoated after formation of grating, which can reduce birefringence phenomena induced by the change of polarization axis due to curing pressure when embedded perpendicularly to reinforcing fibers. Grating 2 was inserted to glass capillary tube whose diameter is slightly larger than that of optical fiber and the tube was bonded at both ends with adhesive. The diameter of jacket-bared optical fiber is 125μm and that of glass capillary tube is about 140 μm. This enables FBG wavelength to shift just by temperature irrespective of mechanical strain applied to the tube embedded in structures.

For acquisition and processing of signals obtained from two FBG sensors, Bragg wavelength detected at photo detector is transformed to electric signal and acquired at DAQ board. And using LabVIEW® program language, temperature and strain can be obtained from Bragg wavelength in real-time. Wavelength-Swept Fiber Laser (WSFL) was used as a broadband source driving FBG sensor system. Also, this system is able to acquire other analogue inputs simultaneously, which was useful for the other experiment that will be mentioned later.

FBG TEMPERATURE SENSOR CALIBRATION

K-Type thermocouple system was constituted and calibrated for reference thermometer to re-calibrate FBG temperature sensor later (grating 2 in Fig.1). In high temperature range (from room temperature to 100 ^{o}C), to reduce the error induced by convection of water, water was heated up to boiling point by an electric heater and then power shut off, temperature from standard thermometer and output voltage were measured as water being cooled down in air. In low temperature range (from room temperature to –196 ^{o}C), three reference materials whose thermal properties like melting point and boiling point are known were used: ice (0 ^{o}C), dry ice (-78.5 ^{o}C), LN2. (-196 ^{o}C). Using these materials, output voltages of thermocouple system were measured. All calibration tests were conducted 3 times and the experimental data were averaged. The other temperature range except measured temperature points was interpolated.

Using calibrated thermocouple system as reference thermometer, FBG temperature sensor was re-calibrated over high and low temperature ranges, respectively. At first, in high temperature range, thermocouple and FBG temperature sensor was put into the oven with being kept within 10 *mm* away and then heated from 20 ^{o}C to 100 ^{o}C at the rate of 1 ^{o}C /minute. Two analogue signals (output voltage and Bragg wavelength) could be obtained simultaneously through thermocouple system and FBG sensor system.

In low temperature range, thermocouple and FBG temperature sensor was attached on the top surface of an aluminum specimen and the specimen was set apart parallel to the surface of LN2 in urethane container and then the container was covered tightly. And data acquisition was accomplished as same as in the high temperature range.

Through FBG temperature calibration tests, the temperature of structures can be measured from Bragg wavelength shift as shown in Fig. 2 [2]. It can be shown that the nonlinearity exists between temperature and wavelength shift in the vicinity of -70 ^{o}C. FBG temperature sensor was used as a reference thermometer in the rest of this research.

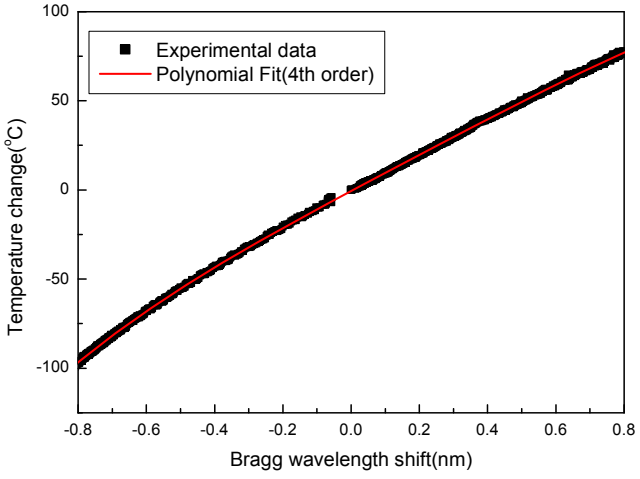

Fig. 2 Bragg wavelength shift vs. △T.

FBG STRAIN SENSOR VERIFICAION

To verify the accuracy of FBG strain sensor in the range of high and low temperature, comparative test with conventional electric strain gauge was performed. Half bridge strain

gauge circuit was made to remove the influence of temperature on strain gauge itself. A dummy gauge was attached on titanium silicate which has very low CTE ($\alpha \approx 0.3\ \mu\varepsilon$).

At the center of aluminum specimen the dimension of which is 50×100×7 *mm*, a FBG strain sensor, a FBG temperature sensor and a strain gauge (EA-13-250BG-120) were attached as shown in Fig. 3. The dummy gage on titanium silicate was located near to active gauge so as to undergo the same temperature environment.

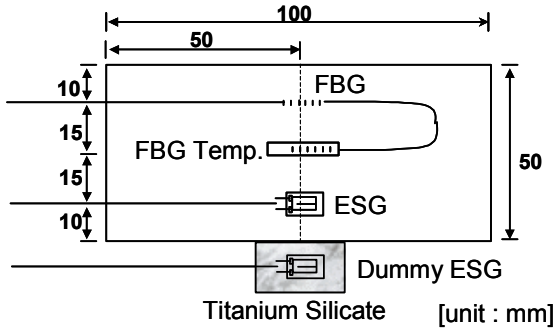

Fig. 3 Aluminum specimen and sensor location for verification test.

Verification in high temperature range (from room temperature to 100 ^{o}C) was performed in the oven, where the aluminum specimen was set on Teflon film to deform freely without friction with the change of temperature. Then, to keep thermal equilibrium, the specimen was heated at the rate of 0.5 ^{o}C /min and the strains with temperature change were obtained from FBG sensor system and temperature from thermocouple system.

In low temperature range (from room temperature to –80 ^{o}C), the verification was performed using LN2 in the urethane vessel. The aluminum specimen was set apart parallel to surface of LN2 and the vessel was sealed up. After thermal equilibrium had been reached, strains of FBG strain sensor and strain gauge were measured as in the same way as high temperature test. By adjusting the level of LN2, final equilibrium temperature was varied and so were strains. In this way we could acquire data at various temperatures. Experimental results showed good agreement between FBG strain sensor and electric strain gauge with maximum error within 4 % as shown in Fig. 4, where 'Theory' means the strain value calculated from CTE of aluminum itself.

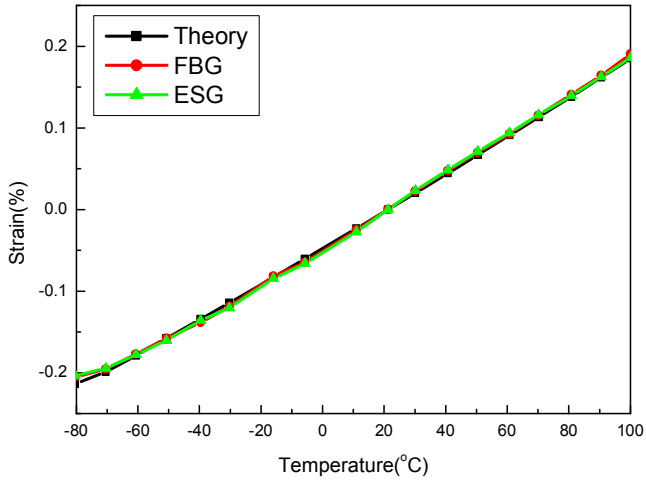

Fig. 4 Results of comparative test between FBG and ESG

MEASUREMENT OF CTE OF COMPOSITE UNDER SPACE ENVIRONMENT WITH AGING

FABRICATION OF COMPOSITE SPECIMEN

The fiber optic sensors for the measurement of temperature and strain in Fig. 1 was embedded into composite specimen to exclude other factors such as vacuum, ultraviolet and so on. The direction of sensors were embedded transverse to reinforcing fibers because the thermal strain in the fiber direction is known to be very small while considerable is that in the transverse direction of the fibers.

The sensor embedding location is shown in Fig. 5. The composite laminated plate is fabricated from HFG-CU-125NS graphite/epoxy prepreg tape and the stacking sequence is $[90_8/\{90\}/90_8]_T$, where {} means optical fiber and the angle in {} is the embedding angle of the optical fiber. Reinforcing ingress/egress tubes were used to protect fiber optic during curing process.

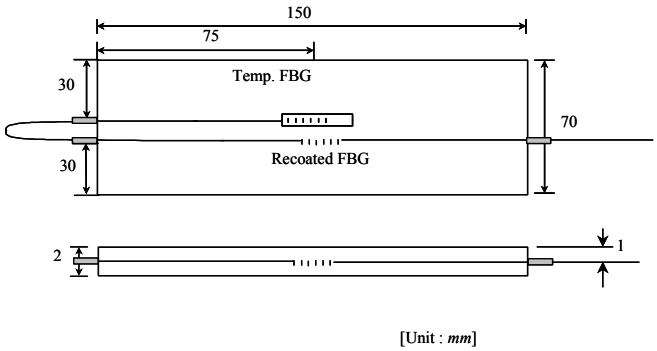

Fig. 5 Composite specimen with FBG sensors

SPACE ENVIRONMENT TEST USING THERMAL VACUUM CHAMBER

Thermal vacuum chamber can simulate low earth orbit (LEO) environment such as vacuum (10^{-6} *Torr*), ultraviolet (wavelength below 200 *nm*) and thermal cycling (-70 ^oC ~ 100 ^oC). After composite specimen in Fig. 5 was set in the thermal vacuum chamber, the LEO environment was simulated. Temperature and strain were measured simultaneously to calculate CTE after 0, 200, 400, 600, 800 and 1000 thermal cycles. 0 cycle means data of 'not aged' specimen, which were acquired from one thermal cycle excluding vacuum and ultraviolet. The CTE curve (T-α curve) was induced from differentiating interpolation function of T-ε curve (temperature-strain) and both ends of T-α curve were cut to eliminate the errors at the end of interpolation line.

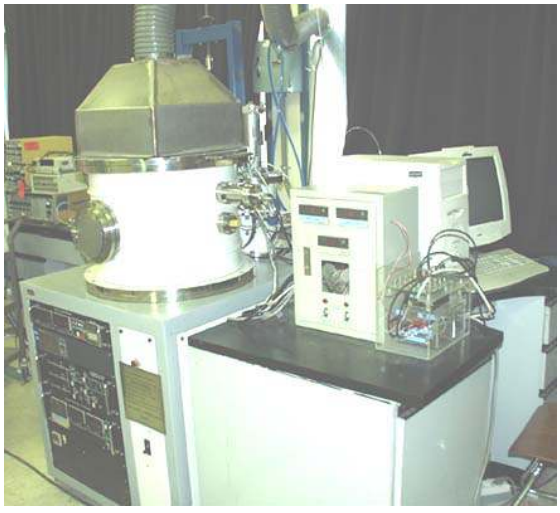

Fig. 6 Thermal vacuum chamber.

The CTE change of composite transverse to reinforcing fibers with space aging cycles is shown in Fig. 7 and Table 1.

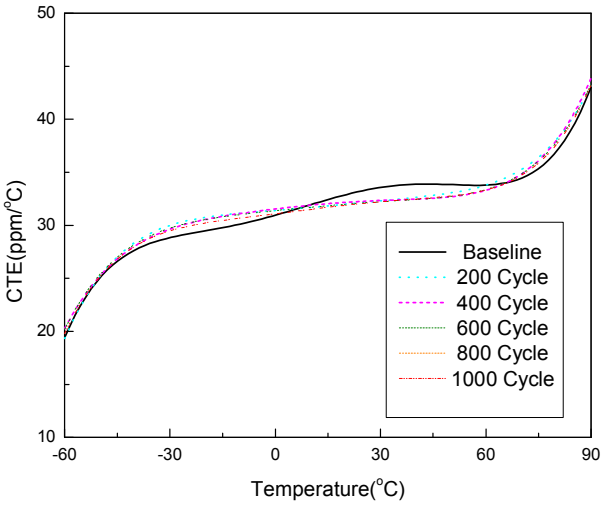

Fig. 7 Coefficient of thermal expansion for transverse direction with aging.

Temp.	baseline	200	400	600	800	1000	change(%)	after 200
−60	19.4	19.3	20.3	20.2	20.2	19.8	2.1	2.4
−40	27.7	28.4	28.1	28.2	28.3	28.0	1.3	−1.3
−20	29.5	30.7	30.5	30.5	30.4	30.2	2.5	−1.7
−10	30.1	31.1	31.1	31.0	30.8	30.7	1.9	−1.4
0	31.0	31.4	31.5	31.4	31.2	31.1	0.4	−1.0
20	32.9	32.0	32.2	32.0	32.0	31.9	−3.0	−0.3
40	33.9	32.6	32.5	32.4	32.5	32.5	−4.1	−0.5
60	33.8	33.8	33.3	33.4	33.3	33.3	−1.4	−1.4
70	34.4	35.2	34.8	34.8	34.7	34.7	0.7	−1.6
90	43.0	43.2	43.9	43.3	43.5	43.2	0.4	0.0

Table 1. The change of CTE with aging (με/°C).

As in the Fig. 6, baseline data is quite different from the others. This result means the composite specimen had not been stabilized until about 200 cycles due to impurities such as moisture or other volatile components. After 200 thermal cycles, as a whole, there was no abrupt change in the CTE of composite. However, CTE shows a little decrease all over the test temperature range. It seems that matrix loss, matrix cracking, outgassing, moisture desorption and so on cause the increase of fiber volume fraction and in turn, decrease of CTE.

CONCLUSION

In this research, fiber optic sensor that has many advantages comparing with conventional thermocouple and strain gauge was embedded into composite material used in the wide fields including aerospace vehicles nowadays. And the fiber optic embedded composite underwent simulated LEO environment such as vacuum, ultraviolet, thermal cycling, etc. As the number

of thermal cycling increased, that is, the space environmental aging proceeded, CTE was acquired by measuring temperature and strain in real-time using FBG sensors. In the pre-test, FBG temperature sensor was calibrated and the reliability of FBG strain sensor was verified by means of comparative test with strain gauge over the experiment temperature range.

It can be established that the fiber optic sensor system can be successfully applied to composite structures and consequently helpful to check the health status of the vehicles under space environment.

REFERENCES

1. P. E. George, H. W. Dursh, “Low Earth Orbit Effects on Organic Composites Flown on The Long Duration Exposure Facility”, *Journal of Advanced Materials*, Vol. 25, No.3, 1994, pp.10-19

2. H. K. Kang, C. Y. Ryu, C. S. Hong, and C. G. Kim, “Simultaneous Measurement of Strain and Temperature of Structures Using Fiber Optic Sensor”, *Journal of Intelligent Material Systems and Structures*, Vol. 12, No.4, 2001, pp. 277-282

3. W. Ecre, I. Latka, R. Willsch, A. Reutlinger, R. Graue, “Fibre Optic Sensor Network for Spacecraft Health Monitoring,” *Measurement Science and Technology*, Vol. 12, No. 7, 2001

4. K. Shigenori, O. Tsuyoshi, T.Nobuo, “Strain and temperature monitoring in composite sandwich panels in space environment”, *Proceedings of SPIE*, Vol. 4185, 2000, pp.126-129.

5. Friebele E.J, Askins C.G et al., “Optical fiber sensors for spacecraft applications”, *Smart materials and structures*, Vol. 8, No. 6, 1999, pp. 813-838.

6. Hugh L. McManus, “Prediction of Thermal Cycling induced matrix cracking”, *Journal of Reinforced Plastics and Composites*”, Vol. 15, 1996, pp.124-140.

7. Cecelia H.Park, Hgh L. McManus, “ Thermally induced damage in composite laminate: Predictive methodology and experimental investigation”, *Composites Science and Technology*, Vol 56, 1996, pp.1209-1219.

8. H. K. Kang, D. H. Kang, C. S. Hong, and C. G. Kim, "Simultaneous Monitoring of Strain and Temperature During and After Cure of Unsymmetric Composite Laminate Using Fiber Optic Sensors," *Smart Materials and Structures*, Vol. 12, No. 1, 2003, pp. 29-35.

9. S. W. James, M. L. Dockney, R. P. Tatam, “Simultaneous independent temperature and strain measurement using in-fibre Brag grating sensors,” *Electronics Letters*, Vol. 32, No. 12, 1133-1134, 1996

10. K. B. Shin, C. G. Kim, C. S. Hong, and H. H. Lee, "Thermal Distortion Analysis of Solar Array including degradation of Composite Materials in Low Earth Orbit Environments," *Composites Part B : Engineering*, Vol. 32, 2001, pp. 271-285.